Functional *mgrA* Influences Genetic Changes within a *Staphylococcus aureus* Cell Population over Time

James Lee,[a,b,c] Miguel Carda-Diéguez,[d] Miglė Žiemytė,[d] Sarah Vreugde,[e] Clare Cooksley,[e] Heidi A. Crosby,[f] Alexander R. Horswill,[f] Alex Mira,[d] Peter S. Zilm,[g] Stephen P. Kidd[a,b,c]

[a]Department of Molecular and Biomedical Sciences, School of Biological Sciences, The University of Adelaide, Adelaide, South Australia, Australia
[b]Research Centre for Infectious Disease (RCID), The University of Adelaide, Adelaide, South Australia, Australia
[c]Australian Centre for Antimicrobial Resistance Ecology (ACARE), The University of Adelaide, Adelaide, South Australia, Australia
[d]Department of Health and Genomics, Center for Advanced Research in Public Health, FISABIO Foundation, Valencia, Spain
[e]Department of Otolaryngology, Head and Neck Surgery, Basil Hetzel Institute, South Australia, Adelaide, Australia
[f]Department of Immunology and Microbiology, University of Colorado School of Medicine, Aurora, Colorado, USA
[g]Adelaide Dental School, The University of Adelaide, Adelaide, South Australia, Australia

ABSTRACT Prolonged survival in the host-bacteria microenvironment drives the selection of alternative cell types in *Staphylococcus aureus,* permitting quasi-dormant sub-populations to develop. These facilitate antibiotic tolerance, long-term growth, and relapse of infection. Small Colony Variants (SCV) are an important cell type associated with persistent infection but are difficult to study *in vitro* due to the instability of the phenotype and reversion to the normal cell type. We have previously reported that under conditions of growth in continuous culture over a prolonged culture time, SCVs dominated a heterogenous population of cell types and these SCVs harbored a mutation in the DNA binding domain of the gene for the transcription factor, *mgrA*. To investigate this specific cell type further, *S. aureus* WCH-SK2-Δ*mgrA* itself was assessed with continuous culture. Compared to the wild type, the *mgrA* mutant strain required fewer generations to select for SCVs. There was an increased rate of mutagenesis within the Δ*mgrA* strain compared to the wild type, which we postulate is the mechanism explaining the increased emergence of SCV selection. The *mgrA* derived SCVs had impeded metabolism, altered MIC to specific antibiotics and an increased biofilm formation compared to non-SCV strain. Whole genomic sequencing detected single nucleotide polymorphisms (SNP) in phosphoglucosamine mutase *glmM* and tyrosine recombinase *xerC*. In addition, several genomic rearrangements were detected which affected genes involved in important functions such as antibiotic and toxic metal resistance and pathogenicity. Thus, we propose a direct link between *mgrA* and the SCV phenotype.

IMPORTANCE Within a bacterial population, a stochastically generated heterogeneity of phenotypes allows continual survival against current and future stressors. The generation of a sub-population of quasi-dormant Small Colony Variants (SCV) in *Staphylococcus aureus* is such a mechanism, allowing for persistent or relapse of infection despite initial intervention seemingly clearing the infection. The use of continuous culture under clinically relevant conditions has allowed us to introduce time to the growth system and selects SCV within the population. This study provides valuable insights into the generation of SCV which are not addressed in standard laboratory generated models and reveals new pathways for understanding persistent *S. aureus* infection which can potentially be targeted in future treatments of persistent *S. aureus* infection.

KEYWORDS Small Colony Variants, *Staphylococcus aureus*, persistence

1

*S*taphylococcus aureus is commonly associated with persistent infections such as prosthetic joint infection (PJI), endocarditis, and diabetic foot infection (DFI) that are recalcitrant to treatment regimens that persist for months or even years (1). This is in part due to the ability of *S. aureus* to survive and adapt to stresses generated from the host or clinical treatment through the formation of alternative cell types (2). Small Colony Variants (SCV) are one such cell type, characterized as slow growing with an altered modified virulence profile (3, 4). SCVs are known to survive intracellularly in different human cell types and these traits result in the evasion of the immune response, intracellular persistence and avoidance of antimicrobials that would otherwise clear actively growing bacteria (5–9). SCV can exist as a minor sub-population within an active infection, and remain undetectable, however, under certain conditions, selective pressures may favor the emergence and dominance of SCV without clinical symptoms suggesting the infection has been cleared. (3, 10, 11). The dynamics of the bacterial/host interaction may then return to one where active cells dominate following the removal of the stress factors causing a relapse of infection (4, 12). These selective pressures may include the immune response, nutrient limitation, and antimicrobial therapeutics (13–17).

Published research on SCVs was originally based on laboratory generated mutants of *S. aureus* that were genetically stable (sSCV). Mutations in the electron transport in *hemB* (16–18) and *menD* (16, 19–21) and thymidine synthesis via *thyA* (22, 23) produced sSCV while other targets included auxotrophism to CO_2 (24, 25), fatty acids (26, 27), chorismite synthesis (28), and selection with gentamicin (17). However, these mutations may not represent all the features *S. aureus* adopts during clinical infection as sSCV have also be shown to be driven by *sigB* (29). Our research proposes a shift in the paradigm from the mechanisms that facilitate selection of SCV. This model hypothesizes that rather than a direct phenotypic switch, SCV appear stochastically within *S. aureus* populations in the absence of selective pressures (5), but emerge when conditions favor their survival while being non-permissive to the active cell types. Stochastic changes within various species of bacteria that permit survival in changing environments have previously been reported (30). These population dynamics would form the basis of relapsing infection by SCV, chorismite synthesis (28) and selection with gentamicin (17). However, these mutations may not be wholly representative of all the features *S. aureus* adopts during the clinical process of infection. There are other pathways that have been shown to be part of the development of SCV, such as that driven by *sigB* (29). Our research investigates an alternate perspective of SCV where we address a shift in the paradigm from the mechanisms that define the switch to a SCV within a cell to the population dynamics which facilitate selection of SCV from a population. This model presents SCV as being able to appear stochastically within *S. aureus* populations during normal growth in the absence of any selective pressures (5), but only being detectable when there are conditions which favor their survival while being non-permissive to the active cell types. Stochastic changes within a microbial population that permit survival in changing environments have previously been reported in various species of bacteria (30). This would suggest that the shift to a population of SCVs during stressful conditions is through selection of stochastically generated SCVs rather than a direct phenotypic switch in response to stress. Consequently, when selective pressures are removed, the population shifts back to the metabolic active normal cell types. These population dynamics would form the basis of relapsing infection by SCV.

An important factor within the host-pathogen interplay during adaptation by bacterial cells critically involves the time-dependent feature of colonization and infection and the associated temporal context for genetic events. Our laboratory has developed a platform for selecting sSCV within a bacterial cell population through prolonged continuous culture under low growth rate conditions that resemble those in the host (31). The methicillin resistant (MRSA) blood isolate *S. aureus* WCH-SK2 when grown under these conditions produced a diversity of cell phenotypes that included an sSCV (31). An important factor within the host-pathogen interplay during adaptation by the

bacterial cell population critically involves the time-dependent feature of colonization and infection and the associated temporal context for genetic events (5, 32–34). Our laboratory has developed a growth platform for selecting sSCV within a bacterial cell population through prolonged continuous culture while in low growth rate conditions that resemble those in the host, and are not growth phase dependent (31). We grew the methicillin resistant (MRSA) blood isolate *S. aureus* WCH-SK2 over a prolonged time frame (up to 180 generations) and produced a diversity of cell phenotypes that included stable SCV (sSCV) (31).

Whole genome sequencing (WGS) of the sSCV revealed specific genetic changes, most notably a single nucleotide polymorphism (SNP) in the DNA binding domain of the global virulence regulator *mgrA* (resulting in protein shift; Arg92Cys) (35). MgrA controls over 300 different genes affecting virulence, antibiotic resistance, (36) regulation of the Agr virulence system (37) and its role has not previously been reported in *S. aureus* SCV. MgrA is associated with the progression of infection in animal models (38, 39), downregulation of cell invasion (40), adhesion to host molecules, and biofilm formation. Whole genome sequencing (WGS) of the WCH-SK2 and its sSCV cells that were generated at the end of the experiment, revealed this phenotype was associated with specific genetic changes, most notably a single nucleotide polymorphism (SNP) in the DNA binding domain of the global virulence regulator *mgrA* (resulting in protein shift; Arg92Cys) (35). MgrA controls over 300 different genes in *S. aureus* and is well-known for affecting virulence and antibiotic resistance (36), and is closely linked with the regulation of the Agr system of virulence (37). MgrA is associated with the progression of infection in animal models (38, 39). The virulence factors affected by MgrA include the upregulation of capsular polysaccharide, leukocidins, and exotoxins, all of which are downregulated in SCVs (41).

Using an *mgrA* knockout, our aim was to use continuous culture to grow WCH-SK2-Δ*mgrA* to investigate the role of *mgrA* in the selection of SCV (31). We have identified the genetic and genomic changes associated with sSCV and their effect on growth, antibiotic resistance, downregulation of cell invasion (40), adhesion to host molecules, and biofilm formation (38, 40, 42, 43). The virulence factors affected by MgrA include the upregulation of capsular polysaccharide, leukocidins, and exotoxins, all of which are downregulated in SCVs (41). The role of *mgrA* had not previously been reported in *S. aureus* SCV. We have now conducted experiments using WCH-SK2-Δ*mgrA* to characterize the role of *mgrA* when grown under clinically relevant conditions in a chemostat. Using an *mgrA* knockout, we observed the effects of beginning a continuous culture with this mutation as the entire bacterial cell population of *S. aureus* under low growth conditions to investigate the role of this gene in the selection of SCV. We therefore grew WCH-SK2-Δ*mgrA* under the same prolonged, controlled growth conditions as previously described to push the cell population to a SCV type (31). We have identified the genetic and genomic changes associated with sSCV and their effect on growth, biofilm formation, and antibiotic resistance.

RESULTS

Continuous culture of WCH-SK2-Δ*mgrA* selects for SCV. A WCH-SK2-Δ*mgrA* clean deletion knockout was generated as previously described (38). WCH-SK2-Δ*mgrA* was cultured in chemically defined media (CDM) in continuous culture over 53 generations (30 d) (Fig. 1a). The maximum growth rate (μ_{max}) of WCH-SK2-Δ*mgrA* in CDM was calculated as $\mu_{max} = 0.338$ h^{-1}. The growth of WCH-SK2-Δ*mgrA* was then limited to 15% of the μ_{max} which is $\mu_{rel} = 0.051$ h^{-1} to give a generation time (T$_g$) of 13.66 h^{-1}. As the number of generations increased, the proportion of SCV cells also increased (%SCV of total colonies [CFU, CFU]/mL). The parental cell type WCH-SK2-Δ*mgrA* produced large, golden colonies when cultured on tryptic soy agar (TSA) (Fig. 1b). Non-pigmented colonies were observed after approximately 6 generations (3 d) and colonies of smaller size were observed after approximately 11 generations (6 d) within the population (Fig. 1c). SCVs first appeared after 16 generations, (9 d) however, these were non-stable
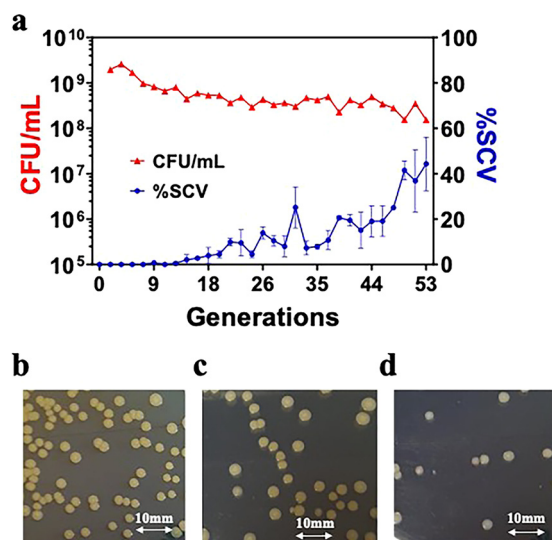
FIG 1 Prolonged growth of WCH-SK2-Δ*mgrA* with limited growth selects for SCV. WCH-SK2-Δ*mgrA* was cultured in CDM within a chemostat over 53 generations of growth (30 d) at a reduced growth rate of $\mu_{rel} = 0.15$. (a) CFU/mL (red, left axis) and % SCV in the population (blue, right axis) was recorded every 24 h. Shown are the cultures plated onto TSA after (b) 3 generations, (c) 16 generations and (d) 50 generations.

and increased in size after subculture on TSA but retained the lack of pigment (Fig. 1d). The only sSCV from the continuous culture experiments was isolated after 50 generations (28 d) which was used in further experiments (WCH-SK2-Δ*mgrA*-SCV). The proportion of SCVs within the population was over 40% after 55 generations (31 d).

Features of the cell type variations were associated with the *mgrA* mutant phenotypic change to SCV. The change in cell type of WCH-SK2-Δ*mgrA* in response to low growth rate ($\mu_{rel} = 0.051$ h^{-1}) was associated with cellular phenotypic differences. SEM imaging of WCH-SK2-Δ*mgrA*-SCV revealed that cells were embedded within an extracellular matrix (Fig. 2). No significant differences were observed between the planktonic growth of WCH-SK2 and WCH-SK2-Δ*mgrA* (as measured by optical density
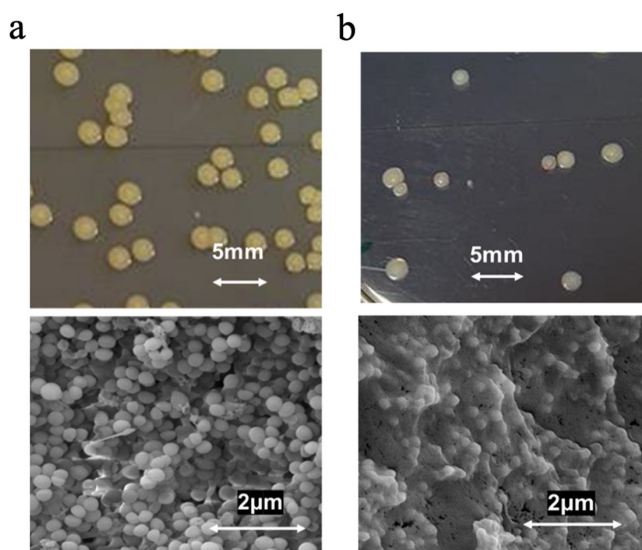

FIG 2 The switch to a SCV in WCH-SK2-Δ*mgrA* is associated with an extracellular matrix. Cell cultures of (a) the parental WCH-SK2-Δ*mgrA* displaying the normal colony type and (b) the SCV isolated after 50 generations were also imaged (bottom panels) using Scanning Electron Microscopy imaging at 20,000x magnification.
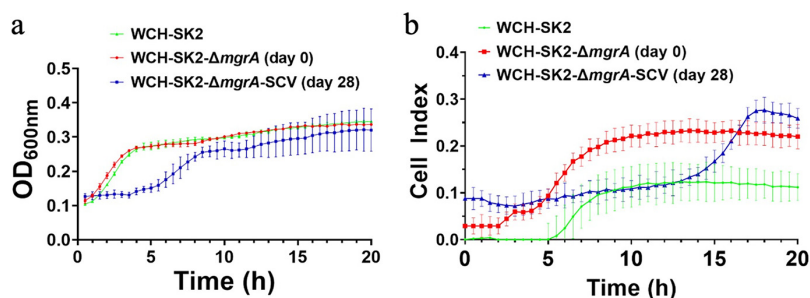
FIG 3 The switch to SCV in WCH-SK2-Δ*mgrA* is associated with changes in growth kinetics and biofilm formation. Both (a) growth was measured spectrophotometrically at 600 nm and (b) biofilm formation was measured using xCELLigence RTCA for WCH-SK2 (green), WCH-SK2-Δ*mgrA* (red) and WCH-SK2-Δ*mgrA*-SCV (blue).

at 600 nm for 20 h). In contrast to these results, the WCH-SK2-Δ*mgrA*-sSCV had an extended lag phase (4 h) compared to the parental cell types (less than 1 h) (Fig. 3a). The mid-exponential phase occurs after 2.25 h for WCH-SK2 andWCH-SK2Δ*mgrA* and 6.7 h for WCH-SK2Δ*mgrA*-SCV (Fig. 3).

Biofilm formation analysis in the impedance-based xCELLigence system enabled the kinetic features of biofilm growth to be measured and compared between strains. Biofilm formation differed in both the kinetics and endpoint quantity between WCH-SK2, WCH-SK2-Δ*mgrA*, and WCH-SK2-Δ*mgrA*-SCV (Fig. 3). Biofilm formation over time displayed distinct phases; lag, exponential phase and stationary phases. Therefore, there is both an indicator of the rate of biofilm formation, as the mid-point of biofilm exponential phase, and the final endpoint value (total biofilm). WCH-SK2-Δ*mgrA*-SCV produced the highest endpoint biofilm followed by WCH-SK2-Δ*mgrA*, and then WCH-SK2, which reached a biofilm mass three times lower than the SCV. Comparing the mid-exponential phase of growth and biofilm formation (Fig. 3) revealed differences in the growth phase dependency of biofilm formation. The mid-exponential phase of biofilm formation for WCH-SK2-Δ*mgrA*-SCV occurred 4 h after WCH-SK2 and WCH-SK2-Δ*mgrA*. In fact, WCH-SK2-Δ*mgrA*-SCV started to form biofilms only around 15 h while WCH-SK2-ΔmgrA reached a similar biofilm mass (Cell Index value of 0.2) already at 7 h.

Comparison of antibiotic MIC between these variants revealed significant changes in their response to penicillin and ciprofloxacin by WCH-SK2-Δ*mgrA*-SCV (Table 1). The parental cell type WCH-SK2 and WCH-SK2-Δ*mgrA* had an unchanged MIC to penicillin, erythromycin, and ciprofloxacin and a minor decrease to gentamicin. WCH-SK2-Δ*mgrA*-SCV demonstrated a 20-fold decrease in resistance to penicillin and an 8-fold increase in resistance to ciprofloxacin (Table 1).

Cell type variants in a *mgrA* mutant is associated with increased mutation frequency. There was a significant difference in the number of generations that selected for SCVs within the population. For WCH-SK2-Δ*mgrA*, SCVs first appeared in continuous culture after 11 generations and an sSCV was isolated after 49 generations (Fig. 1). In the same growth conditions for WCH-SK2, SCVs first appeared after 52 generations and sSCV were isolated after 174 generations (31). We postulated that there was an intrinsic alteration in the permissible level of mutations in the WCH-SK2-Δ*mgrA* strain that

TABLE 1 The switch to a SCV in WCH-SK2-Δ*mgrA* is associated with changes in MIC to antibiotics[a]

Strain	Penicillin (μg/mL)	Gentamicin (μg/mL)	Erythromycin (μg/mL)	Ciprofloxacin (μg/mL)
WCH-SK2	>2000	125	>2000	62.5
WCH-SK2-ΔmgrA	>2000	62.5	>2000	62.5
WCH-SK2-ΔmgrA-SCV	62.5	62.5	1000	500

[a]MIC to antibiotics was determined using broth microdilution assay with 1/2 factor serial dilutions. 2000 μg/mL was the highest concentration antibiotic used in assay and MIC value above this were not identified.

TABLE 2 List of *S. aureus* isolates selected for whole genome sequencing and genome alignment

Isolate name	Colony description	Notes
WCH-SK2-ΔmgrA day 0	Large, pigmented	Parental strain used to inoculate the continuous culture
WCH-SK2-ΔmgrA d28	Large, non-pigmented	Isolated after 50 generations in continuous culture
WCH-SK2-ΔmgrA-SCV d28	SCV	Isolated after 50 generations in continuous culture

allowed mutations that drive SCV formation within the population (31). The rate of mutation was determined by the enumeration of spontaneous mutations in a bacterial cell grown in gentamicin above the MIC. Growth in TSB resulted in no statistically significant differences in the mutation frequency between WCH-SK2 and WCH-SK2-Δ*mgrA*. However, a two-tailed paired T-test revealed the frequency of mutation increased significantly in WCH-SK2-Δ*mgrA* when cultured in CDM (mean of 6.01×10^{-8} mutational events per CFU, *P*-value = 0.006) compared to WCH-SK2 (mean of 7.42×10^{-9} mutation events per CFU, *P*-value = 0.069) (Fig. 4).

Genomic alignments reveal genetic events associated with SCV. The continuous culture of WCH-SK2-Δ*mgrA* created a niche comprised of limited nutrients and hence a low growth rate. In this environment, cell types with differences in metabolic demands may have greater selective fitness, and the imposed slow growth rate would enable slow growing bacteria to increase in proportion. As noted, the SCV phenotype accounted for a significant portion of the population over time (Fig. 2).

After 50 generations (28 days) of WCH-SK2-Δ*mgrA* growing on the chemostat, 2 phenotypes which were clearly differentiated, namely, a large non-pigmented colony and a SCV, were fully sequenced (Table 2). This allowed us to detect single nucleotide polymorphisms (SNPs) and genomic rearrangements (GRAs) i.e., duplications, translocations, insertions, or deletions.

The results revealed a missense mutation in the phosphoglucosamine mutase *glmM* (Gly6Val) and 3 small indels in intergenic regions (Table 3). The non-synonymous mutation at the *glmM* gene was not located in any active or metal binding sites of the protein. GlmM catalyzes the conversion of glucosamine-6-phosphate to glucosamine-1-phosphate for the biosynthesis of the cell wall peptidoglycan. It is important to note that WCH-SK2-Δ*mgrA*-SCV was a single colony obtained from an entire population of
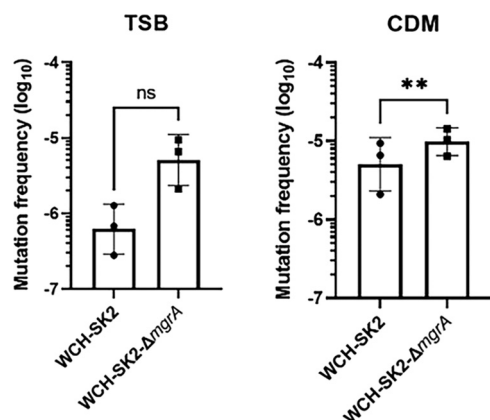

FIG 4 The loss of MgrA activity leads to an increased mutation frequency. The mutation frequency in WCH-SK2 and WCH-SK2-Δ*mgrA* was determined by counting the number of spontaneous mutations after 24 h of growth in (a) TSB and (b) CDM which resulted in resistance against gentamicin. A mutational event was defined as a single colony growing on TSA with gentamicin concentrations above the MIC. The mutation frequency was defined as the number of mutations (CFU/mL on TSA with gentamicin) divided by the total number of cells (CFU/mL on TSA alone). **, = *P*-value < 0.005.

TABLE 3 SNPs detected between WCH-SK2-ΔmgrA d0, WCH-SK2-ΔmgrA d28 and WCH-SK2-ΔmgrA-SCV d28

Genome position	Gene	Nucleotide change	Amino acid change	Product
WCH-SK2-ΔmgrA d0 vs WCH-SK2-ΔmgrA d28[a]				
172237	Non-coding			
177876	Non-coding			
756327	*pre*	502delA	Thr170fs	Plasmid recombination enzyme
775523	Non-coding			
775541	Hypothetical	377_378insGTTTTT		
775544	Hypothetical	375A>G	Glu125Glu	
775619	Hypothetical	300A>T	Val100Val	
777737	*xerC*	81G>A	Gln27Gln	Tyrosine recombinase
777773	*xerC*	45T>C	Ile15Ile	Tyrosine recombinase
777788	*xerC*	30T>C	Ile10Ile	Tyrosine recombinase
2346054	*aroK*	290delA	Lys99fs	Shikimate kinase
2637006	Hypothetical	2318delA	Lys775fs	
2703927	Non-coding			
2703940	Non-coding			
2703955	Non-coding			
2703964	Non-coding			
2703979	Non-coding			
2704093	Non-coding			
WCH-SK2-ΔmgrA d0 vs WCH-SK2-ΔmgrA-SCV d28[b]				
111362	*glmM*	17G>T	Gly6Val	Phosphoglucosamine mutase
172237	Non-coding			
177876	Non-coding			
756327	*pre*	502delA	Thr170fs	Plasmid recombination enzyme
775523	Non-coding			
775541	Hypothetical	377_378insGTTTTT		
775544	Hypothetical	375A>G	Glu125Glu	
777737	*xerC*	81G>A	Gln27Gln	Tyrosine recombinase
777773	*xerC*	45T>C	Ile15Ile	Tyrosine recombinase
777788	*xerC*	30T>C	Ile10Ile	Tyrosine recombinase
1272951	Non-coding			Shikimate kinase
2346054	*aroK*	290delA	Lys99fs	
2637006	Hypothetical	2318delA	Lys775	
WCH-SK2-ΔmgrA d28 vs WCH-SK2-ΔmgrA-SCV d28				
529693	*glmM*	17C>A	Gly6Val	Phosphoglucosamine mutase
592350	Non-coding			
1909645	Non-coding			

[a]large, non-pigmented colony taken after 50 generations.
[b]SCV taken after 50 generations.

cells and may not be representative of all the SCVs present within the population. Genome alignments revealed sections of genome varying between WCH-SK2-Δ*mgrA*-28d and WCH-SK2-Δ*mgrA*-SCV. Notable genes missing in WCH-SK2-Δ*mgrA*-SCV are involved in the SOS response and DNA repair (*gloB*, *recF*), peptidoglycan synthesis (*nagC*), and antibiotic resistance (*mecA*, *mecI*, *tetM*).

Secondly, the complete genomes were compared in order to detect potential Genomic Rearrangements (GRA) that could correspond to added, deleted, or reoriented genomic segments. Only one GRA was found when comparing WCH-SK2-Δ*mgrA* (time zero) and WCH-SK2-Δ*mgrA*-d28. Interestingly, this GRA was not found in WCH-SK2-Δ*mgrA*-SCV. On the other hand, when the WCH-SK2-Δ*mgrA*-SCV strain was compared to the original WCH-SK2-Δ*mgrA*, 54 GRAs were detected (Table 4). Among these GRAs, 46 affected fewer than 10 genes whereas the remaining varied between 14 and 49 genes. In addition, there were 4 "high-divergence" zones where some genes appear to be missing in the SCV genome, and other genes were homologous to the reference ancestral genome but with a

TABLE 4 Genomic Rearrangements (GRAs) in *S. aureus* evolved strains[a]

GRA[b] #	Type of GRA	Encoded genes	# Genes	Mobile/repetitive element	Type of element/Motif
GRA1	Deletion	IS256 family transposase IS256 × 2	2	Transposase	IS256
GRA2	Insertion	ISL3 family transposase IS1181 × 2 Hypothetical protein	3	Transposase	IS1181
GRA3	Deletion	ISL3 family transposase IS256 × 2 Hypothetical protein	3	Transposase	IS256
GRA4	Deletion	IS200/IS605 family transposase ISSep3 Hypothetical protein	2	Transposase	ISSep3
GRA5	Deletion	Hypothetical protein IS256 family transposase IS256	2	Transposase	IS256
GRA6	Insertion	IS200/IS605 family transposase ISSep3	1+1RNA	Transposase + misc RNA	ISSep3 tsr24
GRA7	Insertion	Beta-lactam sensor/signal transducer BlaR1 Beta-lactamase Hypothetical protein × 8 Penicillinase repressor Tyrosine recombinase XerC × 2	14+1RNA	TR + misc RNA + recombinase	tsr24 GAAGAAGAA XerC
GRA8	Deletion	IS256 family transposase IS256 Hypothetical protein	2	Transposase	IS256
GRA9	Deletion	Enterotoxin type A	1+1RNA	Misc RNA	rli28
GRA10	Deletion	ATP-dependent Clp protease proteolytic subunit Chromosome partition protein Smc × 2 Hypothetical protein × 43 Putative HTH-type transcriptional regulator Single-stranded DNA binding protein A Tyrosine recombinase XerC	49	Recombinase	XerC
GRA11	Deletion	ISL3 family transposase IS256 × 2	2	Transposase	IS256
GRA12	Deletion	Hypothetical protein × 0 Tyrosine recombinase XerC	21	TR + recombinase	TTTTACATCATTCCTGGCAT XerC
GRA13	Deletion	ISL3 family transposase IS256 × 2	2	Transposase	IS256
GRA14	Insertion	Arsenate reductase Arsenical pump membrane protein Arsenical pump membrane protein Cadmium resistance transcriptional regulatory protein CadC Cadmium-transporting ATPase Copper-exporting P-type ATPase B × 3 DNA-invertase hin HTH-type transcriptional regulator CysL Hypothetical protein × 21 IS1182 family transposase ISSau3 × 3 IS6 family transposase IS431mec Multicopper oxidase mco Potassium-transporting ATPase ATP-binding subunit Putative ABC transporter ATP-binding protein YknY Putative transposon Tn552 DNA-invertase bin3	40+3RNA	Transposase + misc RNA	ISSau3 tsr24 × 2 fstAT
GRA15	Deletion	ISL3 family transposase IS256 × 2	2	Transposase	IS256
GRA16	Deletion		6	TR	ATCGAGGTGTTTTGTATATAT

TABLE 4 (Continued)

GRA[b] #	# Genes	Type of GRA	Encoded genes	Mobile/repetitive element	Type of element/Motif
			30S ribosomal protein S9; Holliday junction ATP-dependent DNA helicase RuvB; Hypothetical protein × 4		
GRA17	1 + 1RNA	Insertion	ISL3 family transposase IS1181	Transposase + misc RNA	IS1181; sau_5949
GRA18	2	Insertion	IS200/IS605 family transposase ISSep3; Hypothetical protein	Transposase	ISSep3
GRA19	7	Deletion	IS30 family transposase ISSau5; Beta-lactam sensor/signal transducer BlaR1; Beta-lactamase; DNA-invertase hin; Hypothetical protein; ISNCY family transposase ISBli29; Penicillinase repressor	Transposase	ISSau5; ISBli29
GRA20	14	Deletion	IS30 family transposase ISSau5; Hypothetical protein × 12; Translation initiation factor IF-2	Transposase	ISSau5
GRA21	2	Deletion	ISL3 family transposase IS256 × 2	Transposase	IS256
GRA22	1	Deletion	Collagen adhesin		
GRA23	4	Deletion	IS30 family transposase IS1252; Hypothetical protein × 3	Transposase	IS1252
GRA24	45	High-divergence Zone	Beta-lactam sensor/signal transducer MecR1; Bifunctional protein PaaZ; Bleomycin resistance protein; Cadmium resistance transcriptional regulatory protein CadC; Cadmium-transporting ATPase; Glycerophosphodiester phosphodiesterase, cytoplasmic; Hydroxyacylglutathione hydrolase; Hypothetical protein × 26; IS256 family transposase IS256 × 2; IS6 family transposase IS431mec × 2; Kanamycin nucleotidyltransferase; Methicillin resistance regulatory protein MecI; N-acetylglucosamine repressor; PBP2a family beta-lactam-resistant peptidoglycan transpeptidase MecA; Protein McrC; Thiosulfate sulfurtransferase GlpE × 2; Tyrosine recombinase XerC	Transposase+recombinase	IS256; IS431mec; XerC
	14		Hydroxyacylglutathione hydrolase; Hypothetical protein × 11; Putative tRNA-dihydrouridine synthase; Thiosulfate sulfurtransferase GlpE		
GRA25	2 + 1RNA	High-divergence Zone	Hypothetical protein; Replication initiation protein	Misc RNA	S35
	2		Hypothetical protein × 2		
GRA26	2	Deletion	ISL3 family transposase IS256 × 2	Transposase	IS256

(Continued on next page)

TABLE 4 (Continued)

GRA[b] #	# Genes	Type of GRA	Encoded genes	Mobile/repetitive element	Type of element/Motif
GRA27	9	High-divergence Zone	2,3,4,5-tetrahydropyridine-2,6-dicarboxylate N-acetyltransferase	Transposase	IS256
	9		Hypothetical protein × 5		
			IS256 family transposase IS256 × 2		
			2,3,4,5-tetrahydropyridine-2,6-dicarboxylate N-acetyltransferase		
			Hypothetical protein × 8		
GRA28	2	Deletion	IS256 family transposase IS256 × 2	Transposase	IS256
GRA29	1	Deletion	Staphylocoagulase		
GRA30	1	Deletion	Hypothetical protein		
GRA31	1	Deletion	Hypothetical protein	TR	TATTACTTTTACTAGG
GRA32	28	High-divergence Zone	Hypothetical protein × 7		
	17		Type VII secretion system extracellular protein B		
			Type VII secretion system extracellular protein C		
			Type VII secretion system extracellular protein D		
			Type VII secretion system protein EsaE		
			Type VII secretion system protein EsaG × 13		
			Type VII secretion system protein EssC		
			Type VII secretion system protein EssD × 3		
			Hypothetical protein × 12		
			Type VII secretion system protein EsaG × 5		
GRA33	15+1RNA	Insertion	Hypothetical protein × 12	Transposase + misc RNA	ISSau5
			IS30 family transposase ISSau5 × 2		tsr26
			Translation initiation factor IF-2		
GRA34	28	Deletion	ATP-dependent DNA helicase Rep	Transposase+recombinase	ISCth9
			DNA replication and repair protein RecF		ISLgar5
			Hypothetical protein × 22		XerC
			IS21 family transposase ISCth9		
			IS256 family transposase ISLgar5		
			Tetracycline resistance ribosomal protection protein Tet(M)		
			Tyrosine recombinase XerC		
GRA35	1+1RNA	Insertion	ISL3 family transposase IS1181	Transposase + misc RNA	IS1181
					sau_5949
GRA36	2	Deletion	Serine-aspartate repeat-containing protein D	TR	AAAACACCAAAATATAGTTTAGGTGAT TATGTTTGGTACGACAGTAATAAAGA
			Serine-aspartate repeat-containing protein E		
GRA37	2	Deletion in WCH-SK2-ΔmgrA-28d	IS256 family transposase IS256	Transposase	IS256
			Hypothetical protein		
GRA38	2	Deletion	IS256 family transposase IS256	Transposase	IS256
	1	Insertion	Hypothetical protein		
			Hypothetical protein		
GRA39	2	Deletion	IS256 family transposase IS256 × 2	Transposase	IS256
			Hypothetical protein		
GRA40	3	Insertion	ISL3 family transposase IS1181 × 3	Transposase	IS1181
GRA41	1+1RNA	Insertion	ISL3 family transposase IS1181	Transposase + misc RNA	IS1181
					sau-5949
GRA42	3	Deletion	IS256 family transposase IS256 × 2	Transposase	IS256
			Hypothetical protein		
GRA43	25	Deletion		Prophage integrase + TR	TCCCGCCGTCTCCAT

(Continued on next page)

TABLE 4 (Continued)

| GRA[b] #	# Genes	Type of GRA	Encoded genes	Mobile/repetitive element	Type of element/Motif
GRA44	8	Deletion	Putative prophage phiRv2 integrase Hypothetical protein × 22 Iron(3+)-Hydroxamate-binding protein FhuD Tyrosine recombinase XerC × 2 Hypothetical protein × 2 Streptomycin 3"-adenylyltransferase rRNA adenine N-6-methyltransferase 2-methoxy-6-polyprenyl-1,4-benzoquinol methylase, mitochondrial Putative protein YwqG	Misc RNA + recombinase	S35 XerC
GRA45	4	Deletion//insertion	Hypothetical protein × 4		
	4		Hypothetical protein × 4		
GRA46	7	Deletion	Hypothetical protein × 4 IS256 family transposase IS256 × 3	Transposase	IS256
GRA47	3	Deletion	Hypothetical protein IS256 family transposase IS256 × 2	Transposase	IS256
GRA48	2	Deletion	IS256 family transposase IS256 Alpha-hemolysin	Transposase	IS256
GRA49	3	Deletion	Hypothetical protein × 2 IS256 family transposase IS256	Transposase	IS256
GRA50	2+1RNA	Insertion	IS1182 family transposase ISSau3 Hypothetical protein	Transposase + misc RNA	ISSau3 tsr24
GRA51	1	Deletion	Hypothetical protein	TR	CTTTATTT
GRA52	3	Deletion	Hypothetical protein × 2 IS256 family transposase IS256	Transposase	IS256
GRA53	2	Deletion	Hypothetical protein IS256 family transposase IS256	Transposase	IS256
GRA54	3	Deletion	IS256 family transposase IS256 × 2 GlcA/glcB genes antiterminator	Transposase	IS256
GRA55	3+1RNA	Deletion	IS200/IS605 family transposase ISSep3 Hypothetical protein × 2	Transposase + misc RNA	ISSep3 tsr25
GRA56	2	Deletion	IS256 family transposase IS256 × 2	Transposase	IS256
GRA57	1+1RNA	Insertion	ISL3 family transposase IS1181	Transposase + misc RNA	IS1181 sau_5949
GRA58	8	Deletion	Hypothetical protein × 3 rRNA adenine N-6-methyltransferase Streptomycin 3"-adenylyltransferase × 2 Tyrosine recombinase XerC × 2	Recombinase	XerC

[a]Two cell types comprising of a large, non-pigmented producing colony (WCH-SK2-ΔmgrA d28) and a SCV (WCH-SK2-ΔmgrA-SCV d28) were isolated after 50 generations (28 d) in continuous growth. Alignment of whole genome sequences with the ancestral strain were analyzed for genetic GRAs associated with added, deleted or reoriented genomic segments.
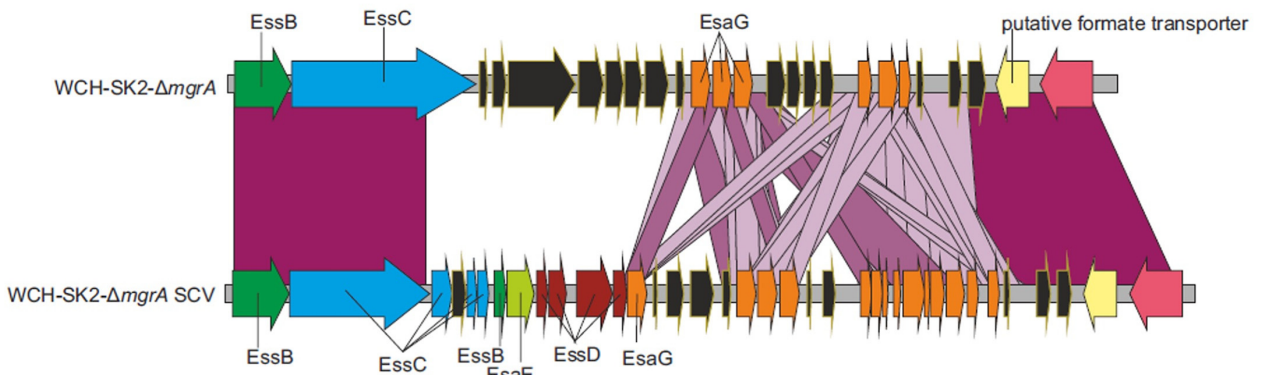
[b]GRA; Genomic Rearrangements.
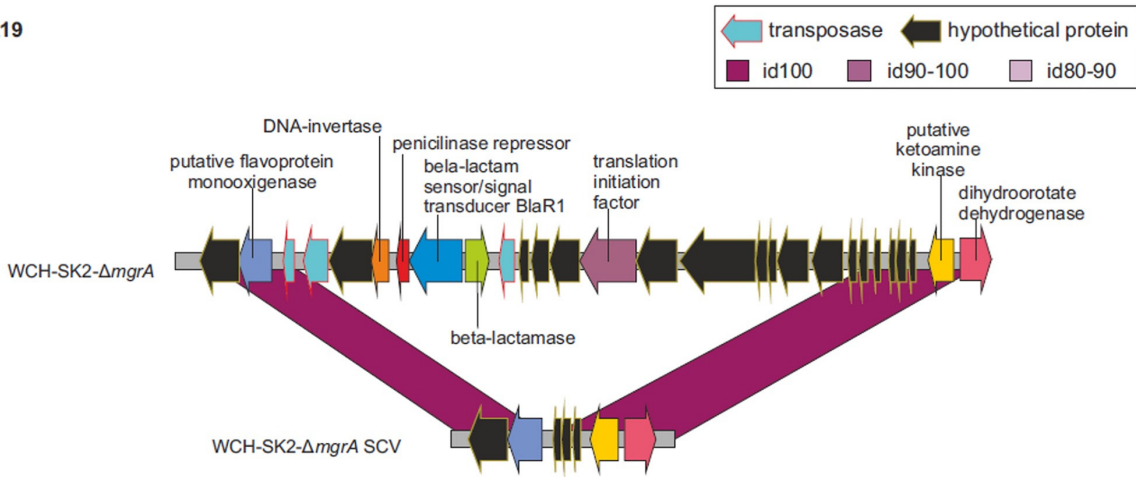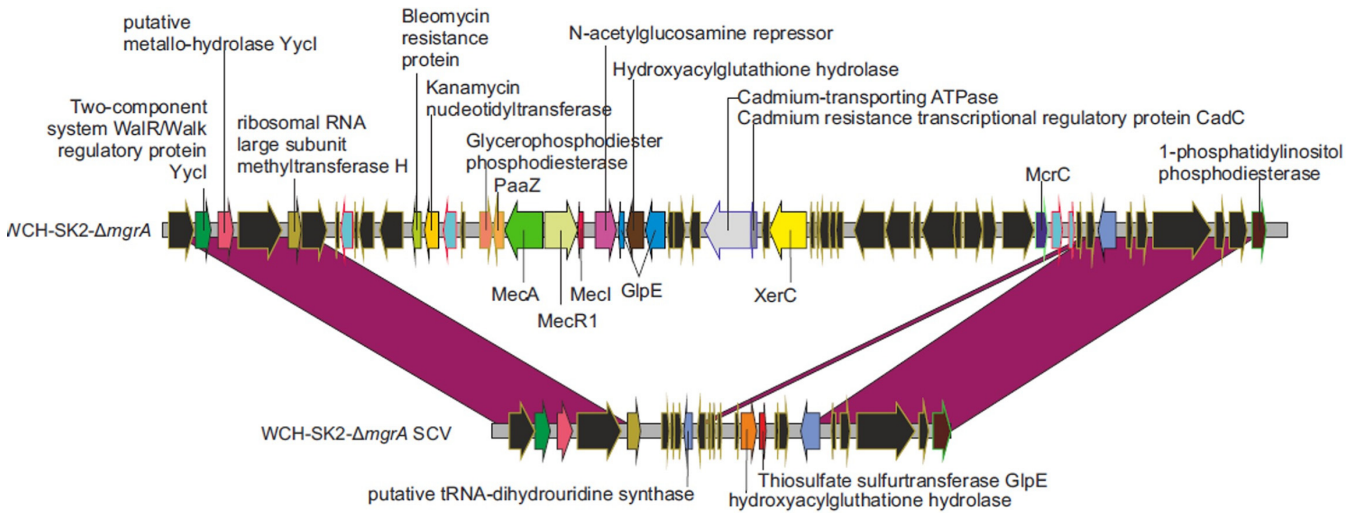
FIG 5 Segments of genome associated with Genomic Rearrangements (GRAs). Three examples of GRAs are shown, representing (A) a case of genomic deletions in the SCV isolate, (B) a region with deletion and insertion of genes in the SCV isolate, and (C) a "high-divergence zone" with the presence of regions in WCH-SK2-Δ*mgrA*-SCV homologous to the parental strain WCH-SK2-Δ*mgrA* but with a low level of DNA sequence similarity.

dramatically low level of sequence similarity (Fig. 5). These highly-divergent regions contained, among others, genes encoding Type VII secretion systems or antibiotic resistance, such as a methicillin resistance regulatory protein (MecI), a kanamycin nucleotidyltransferase, and a bleomycin resistance protein.

To unravel the potential cause of these GRAs, we studied the genomic features
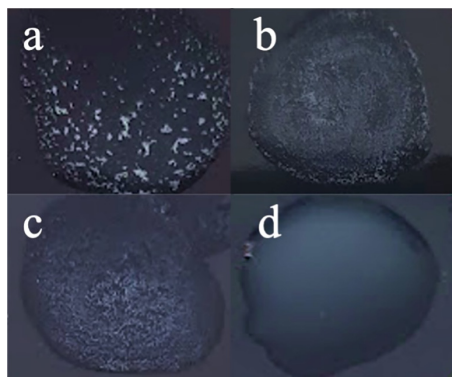
FIG 6 The WCH-SK2Δ*mgrA*-SCV cells are coagulase negative. The presence of coagulase activity was identified in (a) MW2, (b) WCH-SK2Δ*mgrA*-d0, (c) WCH-SK2Δ*mgrA*-d28 (large, non-pigmented colony) and (d) WCH-SK2Δ*mgrA*-SCV-d28. Coagulase positive results are indicated by granular, clumping pattern (a-c) while a coagulase negative result (d) is indicated by a milky background.

present at the edges of the rearranged segments and identified some known to cause genomic instability including transposases, invertases, integrases, recombinases, and/or repetitions at the beginning and the end of the GRAs (Table S3). Interestingly, we detected transposases in 41 cases (71%). In addition, we detected the tyrosine recombinase XerC seven times at adjacent positions, another 7 cases where a repeated DNA sequence was detected at the beginning and the end of the GRA, and 1 case containing a prophage integrase. XerC is a homologue of the *Escherichia coli* tyrosine recombinase which in combination with XerD, separates chromosome dimers which arise during homologous recombination (44). The loss of xerC has been reported to be associated with decreased biofilm formation through increased expression of extracellular nucleases and proteases, and reduced virulence through a decreased accumulation of RNAIII and Agr activation (45). No mobile or repetitive elements were found in 4 cases. In addition, in 14 GRAs, sequences annotated as miscellaneous RNA (also known as non-coding RNA or bacterial introns) were included and we hypothesize that this might also be involved in generating the rearrangements (1, 2). Thus, the origin of most GRAs could be explained by genomic instability imposed by mobile or repetitive genetic elements.

In most cases, inserted/deleted proteins were hypothetical. However, there were some mutated genes with a known function. For example, one of the GRAs affecting both strains had genes involved in the Type VII secretion system. This system has been associated with pathogenesis and the mutation of the entire secretion system or any subunit (EsxA, EssB, EssC, EsxC, EsxB, EsaB, EsaD, or EsaE) has been shown to decrease *S. aureus* virulence (3–8). Other genes that are known to have a role in *S. aureus* infection and were found in the GRAs were enterotoxin type A (10), α-hemolysin (11) or the ATP-dependent Clp protease proteolytic subunit (12). It must be underlined that some of these genes were translocated in the genome but not lost. In addition, staphylocoagulase was found to have several mutations and the automatic annotation by Prokka software split the protein in 3 ORFs, suggesting a potential lack of functionality. A slide coagulase test revealed WCH-SK2-Δ*mgrA*-SCV (d28) was coagulase negative while the WCH-SK2-Δ*mgrA* (d0) and WCH-SK2-Δ*mgrA* (d28) were coagulase positive (Fig. 6). As SCVs have been reported to be very slowly coagulase positive, an additional tube assay was performed allowing a long incubation period. The results were the same (data not shown).

Additionally, mutations in other genes could influence important functions such as antibiotic or toxic metals resistance. For example, the β-lactam sensor/signal transducer BlaR1, a penicillinase repressor, and a β-lactamase were translocated in the WCH-SK2-Δ*mgrA*-28d strain and the β-lactam sensor/signal transducer MecR1 and a PBP2a family β-lactam-resistant peptidoglycan were lost. These genes are important for resistance to the β-lactamase group antibiotics (46). Interestingly, the 3 copies of

streptomycin 3'-adenylyltransferase, which is a gene responsible for streptomycin and/ or spectinomycin resistance, were lost in WCH-SK2-Δ*mgrA*-d28. Furthermore, cadmium resistance transcriptional regulatory protein CadC and cadmium-transporting ATPase were also translocated. On the other side, arsenate reductase, arsenical pump membrane protein, arsenical pump membrane protein, Copper-exporting P-type ATPase B, and multicopper oxidase (*mco*) were lost in WCH-SK2-Δ*mgrA*-SCV.

DISCUSSION

Comparison of the data between WCH-SK2 and WCH-SK2-Δ*mgrA* in continuous culture showed the impact of MgrA on population dynamics in response to prolonged growth in nutrient limited conditions. Wildtype WCH-SK2 required 56 generations (16 d) until SCVs were first observed and an sSCV was first isolated after 192 generations (55 d) (31). The genetic profile of the sSCV included a missense mutation leading to a R92C amino acid in the DNA binding domain of MgrA. MgrA is homologous to MarR in *E. coli,* and previous research identified a R94C SNP in MarR that prevented DNA binding (47). This previously described SNP in MgrA closely aligns to the R94C SNP in WCH-SK2 which implies the SNP in WCH-SK2-SCV would be detrimental to MgrA activity. In addition to a SNP in *mgrA*, WCH-SK2 sSCV after 56 generations also showed the upregulation of Ebh and this was consistent with cells embedded in a proteinaceous extracellular matrix.

In comparison to WCH-SK2, WCH-SK2-Δ*mgrA* took 16 generations (9 d) to reveal SCVs and an sSCV was first isolated after 50 generations (28 d). The loss of MgrA decreased the number of generations required for the formation or selection of SCV and we propose the loss of MgrA function may increase the rate of selection of these alternate cell type through increased ROS production. MgrA has been shown to sense reactive oxygen species (ROS) including hydrogen peroxide and potassium superoxide that results in activation of MgrA targets (48). We speculate that this results in increased intracellular ROS and thereby an increased rate of mutation. This would result in fewer generations being required to accumulate the necessary genetic events that lead to SCV formation and thus allow populations of *S. aureus* to adapt to stresses more efficiently. We did determine the rate of mutation was significantly increased in WCH-SK2-Δ*mgrA* when cultured in CDM compared to the wildtype WCH-SK2. Previous research has identified increased rates of mutagenesis through the SOS DNA repair response was associated with increased frequency of SCV (14). As the same difference in rate of mutation did not occur when cultured in TSB, this rate of mutation is likely dependent on the limited nutrients in CDM. The role of increased ROS in mutation frequency is an avenue for future investigation. Previous research identified glucose, arginine, glutamic acid, and proline as the growth-limiting nutrients for *S. aureus* within this CDM (31). The knockout of *mgrA* alone does not confer the colony type and growth characteristics of SCV in WCH-SK2, but instead creates a population with a greater disposition for genetic events that can result in SCV. In addition, the gene encoding the methylglyoxal detoxification protein *gloB* is missing in WCH-SK2-Δ*mgrA*-SCV. Methylglyoxal is a by-product of metabolism that can create ROS stress and is utilized by the innate immune response to clear pathogens. The loss of methylglyoxal detoxification can increase the presence of ROS, DNA damage and thus mutations through DNA repair mechanisms.

WCH-SK2-Δ*mgrA*-SCV had an impeded growth rate compared to WCH-SK2 and WCH-SK2-Δ*mgrA*. Reduced growth is a defining characteristic of SCV that facilitates persistence during clinical infection. *In silico* analysis of WCH-SK2-Δ*mgrA*-SCV and WCH-SK2-Δ*mgrA* did not detect SNPs in genes that have previously been commonly associated with metabolism in SCV (central carbon metabolism and the electron transport chain). However, GlmM, in addition to DacA and YbbR, are involved in the regulation of the secondary messenger molecule c-di-AMP which controls the osmotic stress response and virulence. Increased intracellular c-di-AMP levels has been shown to result in growth impedance and increased resistance to β-lactams and acid stress

(49–51). DacA is a diadenylate cyclase and the sole producer of c-di-AMP in *S. aureus* (52). Production of c-di-AMP was inhibited when DacA was complexed with GlmM. In addition, YbbR also forms complexes with DacA/GlmM however the function of YbbR on c-di-AMP production is still unknown. Therefore, the loss of *glmM* expression would prevent the repression of c-di-AMP production (or indirect activation of c-di-AMP production). The lack of c-di-AMP production has previously resulted in suppressed growth in complex media such as TSB through the repression of amino acid and osmolyte transporters (53). Additionally, low c-di-AMP levels have been reported to be associated with increased ROS production (53) and so the loss of GlmM activity and increased c-di-AMP may provide another pathway to survive oxidative stresses.

Kinetic readings of biofilm formation using xCELLigence found WCH-SK2-Δ*mgrA*-SCV produced less biofilm at a slower rate but produced a greater biofilm during late stationary phase compared to WCH-SK2-Δ*mgrA*. Studies with an *mgrA* mutant found an increased biofilm formation where early biofilm was dependent on extracellular DNA (43). Additionally, we identified a significantly increased biofilm formation in WCH-SK2-Δ*mgrA* compared to its parental cell type WCH-SK2. The basis for mutations in *mgrA* increasing biofilm formation with reduced clumping is through upregulation of large surface proteins such as Ebh and SasG (38). The loss of *glmM* does not inhibit peptidoglycan synthesis but modifies the properties of the cell wall which reduces the ability for PBP-2 to act against antibiotics (54). This modified cell wall may affect the stability of other cell wall proteins such as Ebh and SasG and the observed changes in extracellular matrix and biofilm formation.

It is interesting to note that contrary to the non-pigmented strain isolated after 28 days of growth in the chemostat, which only had one genomic rearrangement compared to the ancestral WCH-SK2-Δ*mgrA* strain, the SCV isolate generated during the same amount of time had more than 50 genomic rearrangements comprising up to 49 genes. These involved deletions, insertions, translocations and at least 4 regions where genes had undergone extraordinary divergence within 50 generations. Most rearrangements were flanked by mobile or repetitive elements, which are known to generate considerable genomic instability (55). Having this considerable number of mutations, many of which affect genes responsible for the pathogenesis or antibiotic resistance, could be due to cells growing in the absence of a host and in an antibiotic-free environment. SCVs are characterized as slow growing cells with a non-pathogenic virulence profile (3, 4). However, clones carrying these mutations would be expected to be unsuccessful to proliferate in the host or during antibiotic treatment. A plausible explanation to why these are more commonly lost after just a few generations is because they might not be relevant for growing in the chemostat and their loss could contribute to outcompeting other clones with lower fitness. It is remarkable that some regions appeared to have a large sequence divergence compared to the original ancestor. This, together with the large number of genomic regions that vary between WCH-SK2-Δ*mgrA*-28d and WCH-SK2-Δ*mgrA*-SCV but the almost complete genomic stability between WCH-SK2-Δ*mgrA* and WCH-SK2-Δ*mgrA*-28d, suggest that the population of SCVs will be highly heterogenous, favoring the future success of any of the coexisting, highly mutated clones. Heterogenous populations have been reported to maximize the mean fitness of the population in various environments where sub-populations are more fit to survive in unpredictable stressors. Other bacterial species have been reported to create heterogenous populations through a "bet-hedging" strategy, including endospore formation in *Bacillus subtilis* and alteration of metabolism in *Dictyostelium discoiduem*, *E. coli,* and *Lactococcus lactis* (30).

In summary, this study utilized an *mgrA* mutant to demonstrate that a dysfunctional MgrA is an important factor in adaptation to unfavourable conditions by facilitating the generation of different cell types. These cell types include SCV cells which are associated with impeded growth and modulated biofilm formation that result in greater fitness under clinically relevant conditions. While previous research has focused on the direct effects of MgrA on pathogenesis, we identified a potential role of MgrA in the

population dynamics in stressful conditions that may lead to persistent and highly resilient infections.

MATERIALS AND METHODS

Generation of *mgrA* knockout mutations. To construct the *mgrA* deletion plasmid, ~700 bp regions flanking the gene were amplified with primer pairs HC116/HC117 and HC118/119. The products were column purified and fused in a second PCR using primers HC116 and HC119. This fusion product was gel purified, digested with SacI and SalI, and ligated into pJB38 to generate pHC34. This plasmid was electroporated in RN4220, selecting on TSA plates containing Cam at 30°C. The plasmid was then transduced into the MRSA isolate WCH-SK2. Individual colonies were streaked on TSA Cam plates and incubated at 42°C to select for integration into the chromosome. Single colonies were grown in TSB at 30°C and diluted 1:500 in fresh media for four successive days before diluting to 10^{-6} and plating on TSA containing 0.2 μg/mL anhydrotetracycline to select for loss of the plasmid. Colonies were screened for resistance to Cam, and CamS colonies were screened by PCR for deletion of *mgrA*.

Establishing continuous culture conditions. Growth of *S. aureus* was preformed within. Growth was controlled through the flow of chemically defined media medium (CDM, Table S1) into the culture vessel so that the growth rate was relative (μ_{rel}) to the maximum growth rate (0.15% of the μ_{max}). The maximum growth rate was determined by batch culture in CDM within the chemostat vessel. The greatest change in CFU/mL was between 5 and 6 h with a change of 1.4×10^8 CFU/mL. Monod's equation (Equation S1) was used to calculate the maximum growth rate of $\mu_{max} = 0.338h$. The dilution rate (D) was derived from the growth rate (μ) and working volume (V) (Equation S2). To achieve 15% of the maximum growth rate ($\mu_{max} = 0.338$), a flowrate of 25.3 mL/h was required to give a generation time of 13.66 h^{-1}. CDM was prepared as previously described (56) and connected to the chemostat vessel with the inflow of CDM mediated by a peristaltic pump.

Continuous culture of *S. aureus*. Ten milliliters of an overnight culture grown in TSB was washed twice by centrifugation (1900 $\times$ *g*, 4°C, 10 min) and resuspended in 10 mL CDM before inoculated into the chemostat. *S. aureus* was grown by batch culture in a chemostat vessel (Sartorius Biostat B) with a working volume of 500 mL to determine the maximum growth rate. OD_{600} readings were measured at hour intervals, and total cell numbers enumerated ($N_{cells} = OD_{600}$ x 0.8 $\times$ 109) for each sample to determine the maximum growth rate (μ_{max}) and generation time (T_g) using the Monod equation. The greatest change in CFU/mL was between 5 and 6 h with a change of 1.4×10^8 CFU/mL. Monod's equation (Supplementary Equation S1) was used to calculate the maximum growth rate of $\mu_{max} = 0.338h$. The dilution rate (D) was derived from the growth rate (μ) and working volume (V) (Equation S2). To achieve 15% of the maximum growth rate ($\mu_{max} = 0.338$), a dilution rate of 0.05 h^{-1} was achieved with a flowrate of 25.3 mL/h of CDM to the chemostat to give a generation time of 13.66 h^{-1}. The chemostat vessel was kept at pH 7.4 with the addition of ammonia (7.5%). A ring sparger provided aeration directly into the culture medium. Agitation was achieved with a Rushton turbine (6 blade disk impeller) at 250 rpm. Dissolved oxygen concentration was kept constant at 100%. The temperature was kept at 37°C with a double-jacketed glass vessel with thermostat control.

Sample collection and analysis. Aliquots were obtained from the chemostat aseptically with a slip tip syringe connected to a lure-lock sampling tube. To determine colony morphology and CFU/mL, culture broth was serially diluted and plated onto TSA. SCV were classified as non-pigmented colonies with diameter <1mm after 48 h of incubation at 37°C (31). All colonies with a SCV phenotype on TSA was subsequently tested for stability. A SCV was considered stable if it retained the SCV phenotype after 5 subcultures on TSA. Samples of the chemostat were stored by directly centrifuging 5 mL of culture supernatant (1900 $\times$ *g*, 4°C, 10 min) and resuspending in 30% glycerol and stored at −80°C.

Growth kinetics. Growth kinetics assays were performed in 96-well microtiter plates. Cells were incubated in media at 37°C to log phase ($OD_{600} \sim 0.2$). 20 μL of log phase culture was added to a well containing 180 μL of media. Plates were incubated at 37°C for 18 h and OD_{600} readings taken at 30 min intervals with a Sunrise Absorbance Microplate Reader (Tecan).

Determining antibiotic MIC. Antibiotics were serially diluted into TSB by a factor of 1:2. Cells were incubated in TSB at 37°C to log phase ($OD_{600} \sim 0.2$). 20 μL of log phase culture was added to wells containing 180 μL TSB with antibiotic. Cultures were incubated at 37°C for 18 h and OD_{600} readings were taken. Cultures were serially diluted to determine CFU/mL. MIC was determined to be the lowest concentration of antibiotic which resulted in no visual bacterial growth and change in OD_{600}.

Real-time xCELLigence biofilm assay. Real-time biofilm assays were performed with an xCELLigence RTCA (ACEA Biosciences) as previously described (57, 58). Biofilm assay was performed in 16-well ePlates (ACEA Biosciences). 150 μL of CDM was placed into each well and sterile distilled water was placed into the surrounding evaporation control troughs as recommended by the manufacturers. The plate was inserted into the RTCA Plate Analyzer and placed inside a 37°C incubator for 30 min. Bacteria were grown separately to log phase ($OD_{600} \sim 0.2$) and 50 μL was added to ePlate wells in triplicate. Impedance readings were taken at 15 min for 20 h. Cell-sensor impedance was expressed as an arbitrary unit called cell index (CI) according to the manufacturer's instructions. CI at a time point was defined as Z_n-Z_b where Z_n is the cell-electrode impedance of the well that contains the cells and Z_b is the background impedance with media alone. CI values have been shown to correlate with total biofilm mass in *S. aureus* (58).

Coagulase test. Presence of coagulase activity was identified using Remel Coagulase Plasma test tube test as well as the Staphaurex Latex Agglutination Kit (Thermo Scientific) according to manufacturer's protocols.

Rate of mutation (mutation frequency). *S. aureus* cells were incubated overnight in 5 mL of TSB at 37°C. Approximately 1×10^6 cells were inoculated into a series of five 50 mL tubes with 5 mL of fresh TSB. Cultures were incubated at 37°C for 18 h and CFU/mL was enumerated by serial dilution. Cultures were centrifuged ($1900 \times g$, 4°C, 10 min), supernatant was discarded, and cells were resuspended in 100 μL of sterile PBS. Cell suspensions were plated out onto TSA containing gentimicin at a concentration above the MIC for each strain. Colonies which grew on the selective media were defined as a mutational event. The mutation frequency was defined as the proportion of mutational events over the total CFU in the culture.

Scanning electron microscopy (SEM). Cells were filtered through a 0.2 μm Milipore filter paper and fixed with a fixative solution (4% paraformaldehyde, 1.25% glutaraldehyde, 4% sucrose in PBS). Filters were washed twice with 4% sucrose in PBS, post-fixed with 0.1% osmium tetraoxide for 60 min and washed twice with 4% sucrose in PBS. Cells were dehydrated with a series of two 10 min ethanol washes, each in 70%, 90% and 100% ethanol solutions. Cells were dried in a 1:1 mix HMDS and 100% ethanol for 20 min and then in HMDS for 15 min. Samples were mounted onto titanium stubs and coated with 2 mm platinum. Images were taken using a Phillips XL30 FEG scanning electron microscope (Adelaide Microscopy).

Whole genome sequencing. Whole genomic DNA was extracted and purified using Qiagen Genomic-tip 500/G columns (Qiagen) according to manufacturer protocols. Quality and quantity of genomic DNA was determined using FEMTO Pulse (SA Pathology). Genomes were sequenced using PacBio SMRT (Single Molecule Real Time), sequencing performed by the Ramciotti Centre for Genomics (Sydney, Australia) or an Oxford Nanopore MinION device. The MinION library construction and sequencing were performed by FISABIO University of Valencia's sequencing service, using the Oxford Nanopore PCR barcoding kit following the manufacturer's instructions. For this, we combined NextSeq (Illumina) with Minion (Oxford Nanopore) technologies to obtain complete, fully-closed genomes of WCH-SK2-Δ*mgrA*-d28 (the non-pigmented strain) and WCH-SK2-Δ*mgrA*-SCV. Briefly, an average of 3.7 million reads of 150 bp of length sequenced by NextSeq were combined with 150,000 reads of 9.7 ± 0.5 Kbp of length sequenced with Minion technology (Oxford Nanopore Technology) per genome. Consequently, genomes were closed with >500x coverage, where detected polymorphisms could unequivocally be assigned to mutations and not be derived from sequencing errors. Genomes sequencings have been submitted to the BioProject database (as Biosamples): PRJNA821238.

Bioinformatics analysis. Annotation of complete genomes was achieved using Prokka v1.14.6. Virulence factors were identified using VFanalyzer, an automatic pipeline analysis to screen FASTA sequences against the VFanalyzer database for known and/or potential virulence factors in a genome. Antibiotic resistances were identified using the Comprehensive Antibiotic Resistance Database (CARD) and ResFinder 4.0 which uses BLAST to annotate resistance genes and Resistance Gene Identifier (RGI) to detect chromosomal mutations to leading to antibiotic resistance. Genes involved in metabolism were identified using BlastKOALA KEGG annotation tool which annotates genes within a FASTA sequence based on their score against the KEGG genes database. MUMmer v3.0, an open software package which allows rapid alignments of FASTA sequences and has a SNP detection pipeline to identify all SNPs in regions of sequence similarity. Mobile genetic elements were identified by pipelining the whole genome FASTA sequences through relevant databases using PHAST (prophage), ISfinder, (insertion sequences) IslandViewer (genomic islands) and SCCmec Finder 1.2 (SCCmec Type).

SUPPLEMENTAL MATERIAL

Supplemental material is available online only.

SUPPLEMENTAL FILE 1, PDF file, 0.1 MB.

REFERENCES

1. Tong SY, Davis JS, Eichenberger E, Holland TL, Fowler VG, Jr. 2015. *Staphylococcus aureus* infections: epidemiology, pathophysiology, clinical manifestations, and management. Clin Microbiol Rev 28:603–661. https://doi.org/10.1128/CMR.00134-14.
2. Tuchscherr L, Medina E, Hussain M, Volker W, Heitmann V, Niemann S, Holzinger D, Roth J, Proctor RA, Becker K, Peters G, Loffler B. 2011. *Staphylococcus aureus* phenotype switching: an effective bacterial strategy to escape host immune response and establish a chronic infection. EMBO Mol Med 3:129–141. https://doi.org/10.1002/emmm.201000115.
3. Proctor RA, Van Langevelde P, Kristjansson M, Maslow JN, Arbeit RD. 1995. Persistent and relapsing infections associated with small-colony variants of *Staphylococcus aureus*. Clin Infect Dis 20:95–102. https://doi.org/10.1093/clinids/20.1.95.
4. Proctor RA, von Eiff C, Kahl BC, Becker K, McNamara P, Herrmann M, Peters G. 2006. Small colony variants: a pathogenic form of bacteria that facilitates persistent and recurrent infections. Nat Rev Microbiol 4:295–305. https://doi.org/10.1038/nrmicro1384.
5. Edwards AM. 2012. Phenotype switching is a natural consequence of *Staphylococcus aureus* replication. J Bacteriol 194:5404–5412. https://doi.org/10.1128/JB.00948-12.
6. von Eiff C, Peters G, Becker K. 2006. The small colony variant (SCV) concept-the role of staphylococcal SCVs in persistent infections. Injury 37: S26–S33. https://doi.org/10.1016/j.injury.2006.04.006.
7. Garcia LG, Lemaire S, Kahl BC, Becker K, Proctor RA, Denis O, Tulkens PM, Van Bambeke F. 2013. Antibiotic activity against small-colony variants of *Staphylococcus aureus*: Review of in vitro, animal and clinical data. J Antimicrob Chemother 68:1455–1464. https://doi.org/10.1093/jac/dkt072.
8. Proctor RA, Kahl B, Von Eiff C, Vaudaux PE, Lew DP, Peters G. 1998. Staphylococcal small colony variants have novel mechanisms for antibiotic resistance. Clin Infect Dis 27:S68–S74. https://doi.org/10.1086/514906.

9. Forbes S, Latimer J, Bazaid A, McBain AJ. 2015. Altered competitive fitness, antimicrobial susceptibility, and cellular morphology in a triclosan-induced small-colony variant of *Staphylococcus aureus*. Antimicrob Agents Chemother 59:4809–4816. https://doi.org/10.1128/AAC.00352-15.

10. Kahl BC, Herrmann M, Everding AS, Koch HG, Becker K, Harms E, Proctor RA, Peters G. 1998. Persistent infection with small colony variant strains of *Staphylococcus aureus* in patients with cystic fibrosis. J Infect Dis 177: 1023–1029. https://doi.org/10.1086/515238.

11. Von Eiff C, Becker K, Metze D, Lubritz G, Hockmann J, Schwarz T, Peters G. 2001. Intracellular persistence of *Staphylococcus aureus* small-colony variants within keratinocytes: A cause for antibiotic treatment failure in a patient with Darier's disease. Clin Infect Dis 32:1643–1647. https://doi.org/10.1086/320519.

12. Kittinger C, Toplitsch D, Folli B, Landgraf LM, Zarfel G. 2019. Phenotypic stability of *Staphylococcus aureus* small colony variants (SCV) isolates from cystic fibrosis (CF) patients. IJERPH 16:1940. https://doi.org/10.3390/ijerph16111940.

13. Painter KL, Strange E, Parkhill J, Bamford KB, Armstrong-James D, Edwards AM. 2015. *Staphylococcus aureus* adapts to oxidative stress by producing H_2O_2 resistant small-colony variants via the SOS response. Infect Immun 83: 1830–1844. https://doi.org/10.1128/IAI.03016-14.

14. Vestergaard M, Paulander W, Ingmer H. 2015. Activation of the SOS response increases the frequency of small colony variants. BMC Res Notes 8:749. https://doi.org/10.1186/s13104-015-1735-2.

15. Batko IZ, Flannagan RS, Guariglia-Oropeza V, Sheldon JR, Heinrichs DE. 2021. Heme-dependent siderophore utilization promotes iron-restricted growth of the staphylococcus aureus hemB small-colony variant. J Bacteriol 203:e00458-21. https://doi.org/10.1128/JB.00458-21.

16. Schaaff F, Bierbaum G, Baumert N, Bartmann P, Sahl HG. 2003. Mutations are involved in emergence of aminoglycoside-induced small colony variants of *Staphylococcus aureus*. Int J Med Microbiol 293:427–435. https://doi.org/10.1078/1438-4221-00282.

17. Balwit JM, van Langevelde P, Vann JM, Proctor R. 1994. Gentamicin-resistant menadione and hemin auxotrophic *Staphylococcus aureus* persist within cultured endothelial cells. J Infect Dis 170:1033–1037. https://doi.org/10.1093/infdis/170.4.1033.

18. Von Eiff C, Heilmann C, Proctor R, Woltz C, Peters G, Götz F. 1997. A Site-directed *Staphylococcus aureus hemB* mutant is a small colony variant which persists intracellularly. J Bacteriol 179:4706–4712. https://doi.org/10.1128/jb.179.15.4706-4712.1997.

19. Lannergård J, von Eiff C, Sander G, Cordes T, Seggewiss J, Peters G, Proctor RA, Becker K, Hughes D. 2008. Identification of the genetic basis for clinical menadione-auxotrophic small-colony variant isolates of *Staphylococcus aureus*. Antimicrob Agents Chemother 52:4017–4022. https://doi.org/10.1128/AAC.00668-08.

20. Pader V, James EH, Painter KL, Wigneshweraraj S, Edwards AM. 2014. The agr quorum-sensing system regulates fibronectin binding but not hemolysis in the absence of a functional electron transport chain. Infect Immun 82:4337–4347. https://doi.org/10.1128/IAI.02254-14.

21. Dean MA, Olsen RJ, Wesley LS, Rosato AE, Musser JM. 2014. Identification of point mutations in clinical *Staphylococcus aureus* strains that produce small-colony variants auxotrophic for menadione. Infect Immun 82: 1600–1605. https://doi.org/10.1128/IAI.01487-13.

22. Besier S, Ludwig A, Ohlsen K, Brade V, Wichelhaus TA. 2007. Molecular analysis of the thymidine-auxotrophic small colony variant phenotype of *Staphylococcus aureus*. Int J Med Microbiol 297:217–225. https://doi.org/10.1016/j.ijmm.2007.02.003.

23. Chatterjee I, Kriegeskorte A, Fischer A, Deiwick S, Theimann N, Proctor RA, Peters G, Herrmann M, Kahl BC. 2008. In vivo mutations of thymidylate synthase (encoded by *thyA*) are responsible for thymidine dependency in clinical small-colony variants of *Staphylococcus aureus*. J Bacteriol 190: 834–842. https://doi.org/10.1128/JB.00912-07.

24. Gómez-González C, Acosta J, Villa J, Barrado L, Sanz F, Orellana MÁ, Otero JR, Chaves F. 2010. Clinical and molecular characteristics of infections with CO_2-dependent small-colony variants of *Staphylococcus aureus*. J Clin Microbiol 48:2878–2884. https://doi.org/10.1128/JCM.00520-10.

25. Thomas ME. 1955. Studies on a CO_2-dependent *Staphylococcus*. J Clin Pathol 8:288–291. https://doi.org/10.1136/jcp.8.4.288.

26. Bazaid AS, Forbes S, Humphreys GJ, Ledder RG, O'Cualain R, McBain AJ. 2018. Fatty acid supplementation reverses the small colony variant phenotype in triclosan-adapted *Staphylococcus aureus*: genetic, proteomic and phenotypic analyses. Sci 8:1–9.

27. Schleimer N, Kaspar U, Drescher M, Seggewiß J, von Eiff C, Proctor RA, Peters G, Kriegeskorte A, Becker K. 2018. The energy-coupling factor transporter module EcfAA'T, a novel candidate for the genetic basis of fatty acid-auxotrophic small-colony variants of *Staphylococcus aureus*. Front Microbiol 9:1863.

28. Zhang P, Wright JA, Osman AA, Nair SP. 2017. An aroD cchre mutation results in a *Staphylococcus aureus* small colony variant that can undergo phenotypic switching via two alternative mechanisms. Front Microbiol 8:1001. https://doi.org/10.3389/fmicb.2017.01001.

29. Tuchscherr L, Löffler B. 2016. *Staphylococcus aureus* dynamically adapts global regulators and virulence factor expression in the course from acute to chronic infection. Curr Genet 62:15–17. https://doi.org/10.1007/s00294-015-0503-0.

30. Grimbergen AJ, Siebring J, Solopova A, Kuipers OP. 2015. Microbial bet-hedging: the power of being different. Curr Opin Microbiol 25:67–72. https://doi.org/10.1016/j.mib.2015.04.008.

31. Bui LMG, Hoffmann P, Turnidge JD, Zilm PS, Kidd SP. 2015. Prolonged growth of a clinical *Staphylococcus aureus* strain selects for a stable small-colony-variant cell type. Infect Immun 83:470–481. https://doi.org/10.1128/IAI.02702-14.

32. Kalinka J, Hachmeister M, Geraci J, Sordelli D, Hansen U, Niemann S, Oetermann S, Peters G, Löffler B, Tuchscherr L. 2014. *Staphylococcus aureus* isolates from chronic osteomyelitis are characterized by high host cell invasion and intracellular adaptation, but still induce inflammation. Int J Med Microbiol 304:1038–1049. https://doi.org/10.1016/j.ijmm.2014.07.013.

33. Goerke C, Wolz C. 2010. Adaptation of *Staphylococcus aureus* to the cystic fibrosis lung. Int J Med Microbiol 300:520–525. https://doi.org/10.1016/j.ijmm.2010.08.003.

34. Tuchscherr L, Pöllath C, Siegmund A, Deinhardt-Emmer S, Hoerr V, Svensson CM, Figge MT, Monecke S, Löffler B. 2019. Clinical *S. aureus* isolates vary in their virulence to promote adaptation to the host. Toxins 11: 135. https://doi.org/10.3390/toxins11030135.

35. Bui LMG, Kidd SP. 2015. A full genomic characterization of the development of a stable small colony variant cell-type by a clinical *Staphylococcus aureus* strain. Infect Genet Evol 36:345–355. https://doi.org/10.1016/j.meegid.2015.10.011.

36. Luong TT, Dunman PM, Murphy E, Projan SJ, Lee CY. 2006. Transcription profiling of the *mgrA* regulon in *Staphylococcus aureus*. J Bacteriol 188: 1899–1910. https://doi.org/10.1128/JB.188.5.1899-1910.2006.

37. Ingavale SS, van Wamel W, Luong TT, Lee CY, Cheung AL. 2005. Rat/MgrA, a regulator of autolysis, is a regulator of virulence genes in *Staphylococcus aureus*. Infect Immun 73:1423–1431. https://doi.org/10.1128/IAI.73.3.1423-1431.2005.

38. Crosby HA, Schlievert PM, Merriman JA, King JM, Salgado-Pabon W, Horswill AR. 2016. The *Staphylococcus aureus* global regulator MgrA modulates clumping and virulence by controlling surface protein expression. PLoS Pathog 12:e1005604. https://doi.org/10.1371/journal.ppat.1005604.

39. Jonsson IM, Lindholm C, Luong TT, Lee CY, Tarkowski A. 2008. *mgrA* regulates staphylococcal virulence important for induction and progression of septic arthritis and sepsis. Microbes Infect 10:1229–1235. https://doi.org/10.1016/j.micinf.2008.07.026.

40. Lei MG, Gudeta DD, Luong TT, Lee CY. 2019. MgrA negatively impacts *Staphylococcus aureus* invasion by regulating capsule and FnbA. Infect Immun 87. https://doi.org/10.1128/IAI.00590-19.

41. Lee J, Zilm PS, Kidd SP. 2020. Novel research models for *Staphylococcus aureus* small colony variants (SCV) development: co-pathogenesis and growth rate. Front Microbiol 11:321.

42. Kwiecinski JM, Crosby HA, Valotteau C, Hippensteel JA, Nayak MK, Chauhan AK, Schmidt EP, Dufrêne YF, Horswill AR. 2019. *Staphylococcus aureus* adhesion in endovascular infections is controlled by the ArlRS–MgrA signaling cascade. PLoS Pathog 15:e1007800. https://doi.org/10.1371/journal.ppat.1007800.

43. Trotonda MP, Tamber S, Memmi G, Cheung AL. 2008. MgrA represses biofilm formation in *Staphylococcus aureus*. Infect Immun 76:5645–5654. https://doi.org/10.1128/IAI.00735-08.

44. Castillo F, Benmohamed A, Szatmari G. 2017. Xer site specific recombination: double and single recombinase systems. Front Microbiol 8:453. https://doi.org/10.3389/fmicb.2017.00453.

45. Atwood DN, Beenken KE, Loughran AJ, Meeker DG, Lantz TL, Graham JW, Spencer HJ, Smeltzer MS. 2016. XerC contributes to diverse forms of *Staphylococcus aureus* infection via agr-dependent and agr-independent pathways. Infect Immun 84:1214–1225. https://doi.org/10.1128/IAI.01462-15.

46. Peacock SJ, Paterson GK. 2015. Mechanisms of methicillin esistance in *Staphylococcus aureus*. Annu Rev Biochem 84:577–601. https://doi.org/10.1146/annurev-biochem-060614-034516.

47. Alekshun MN, Kim YS, Levy SB. 2000. Mutational analysis of MarR, the negative regulator of marRAB expression in *Escherichia coli*, suggests the presence of two regions required for DNA binding. Mol Microbiol 35:1394–1404. https://doi.org/10.1046/j.1365-2958.2000.01802.x.

48. Chen PR, Bae T, Williams WA, Duguid EM, Rice PA, Schneewind O, He C. 2006. An oxidation-sensing mechanism is used by the global regulator MgrA in *Staphylococcus aureus*. Nat Chem Biol 2:591–595. https://doi.org/10.1038/nchembio820.

49. Bowman L, Zeden MS, Schuster CF, Kaever V, Gründling A. 2016. New insights into the cyclic di-adenosine monophosphate (c-di-AMP) degradation pathway and the requirement of the cyclic dinucleotide for acid stress resistance in *Staphylococcus aureus**. J Biol Chem 291:26970–26986. https://doi.org/10.1074/jbc.M116.747709.

50. Corrigan RM, Bellows LE, Wood A, Gründling A. 2016. ppGpp negatively impacts ribosome assembly affecting growth and antimicrobial tolerance in Gram-positive bacteria. Proc Natl Acad Sci U S A 113:E1710–E1719. https://doi.org/10.1073/pnas.1522179113.

51. Dengler V, McCallum N, Kiefer P, Christen P, Patrignani A, Vorholt JA, Berger-Bächi B, Senn MM. 2013. Mutation in the C-Di-AMP cyclase dacA affects fitness and resistance of methicillin resistant *Staphylococcus aureus*. PLoS One 8:e73512. https://doi.org/10.1371/journal.pone.0073512.

52. Tosi T, Hoshiga F, Millership C, Singh R, Eldrid C, Patin D, Mengin-Lecreulx D, Thalassinos K, Freemont P, Gründling A. 2019. Inhibition of the *Staphylococcus aureus* c-di-AMP cyclase DacA by direct interaction with the phosphoglucosamine mutase GlmM. PLoS Pathog 15:e1007537. https://doi.org/10.1371/journal.ppat.1007537.

53. Zeden MS, Schuster CF, Bowman L, Zhong Q, Williams HD, Gründling A. 2018. Cyclic di-adenosine monophosphate (c-di-AMP) is required for osmotic regulation in *Staphylococcus aureus* but dispensable for viability in anaerobic conditions. J Biol Chem 293:3180–3200. https://doi.org/10.1074/jbc.M117.818716.

54. Glanzmann P, Gustafson J, Komatsuzawa H, Ohta K, Berger-Bächi B. 1999. glmM operon and methicillin-resistant glmM suppressor mutants in *Staphylococcus aureus*. Antimicrob Agents Chemother 43:240–245. https://doi.org/10.1128/AAC.43.2.240.

55. Alibayov B, Baba-Moussa L, Sina H, Zdeňková K, Demnerová K. 2014. *Staphylococcus aureus* mobile genetic elements. Mol Biol Rep 41:5005–5018. https://doi.org/10.1007/s11033-014-3367-3.

56. Hussain M, Hastings JGM, White PJ. 1991. A chemically defined medium for slime production by coagulase-negative staphylococci. J Med Microbiol 34:143–147. https://doi.org/10.1099/00222615-34-3-143.

57. Abrantes P, Africa CWJ. 2020. Measuring *Streptococcus mutans*, *Streptococcus sanguinis* and *Candida albicans* biofilm formation using a real-time impedance-based system. J Microbiol Methods 169:105815. https://doi.org/10.1016/j.mimet.2019.105815.

58. Ferrer MD, Rodriguez JC, Álvarez L, Artacho A, Royo G, Mira A. 2017. Effect of antibiotics on biofilm inhibition and induction measured by real-time cell analysis. J Appl Microbiol 122:640–650. https://doi.org/10.1111/jam.13368.